Journal of Operation and Automation in Power Engineering

vol. XX, no. XX, Dec. 2022, Pages: XXXX (Proofed)

http://joape.uma.ac.ir

Enhancing Smart Grid Systems: A Novel Mathematical Approach for Optimized Fault Recovery and Improved Energy Efficiency

*A.Y. Dewi[1], M.Y. Arabi[2, *], Z.F. Al-Lami[3], M.M. Abdulhasan[4], A.S. Ibrahim[5], R. Sattar[6], D.A. Lafta[7], B.A. Usmanovich[8], D. Abdullah[9], and Y. Yerkin[10]*

[1] *Department of Electrical Engineering, Institut Technologi Padang, Indonesia.*
[2] *Al-Hadi University College, 10011, Baghdad, Iraq.*
[3] *Al-Manara College for Medical Sciences, Maysan, Iraq.*
[4] *Department of Medical Laboratories Technology, AL-Nisour University College, Baghdad, Iraq.*
[5] *College of Computer, National University of Science and Technology, Dhi Qar, Iraq.*
[6] *Al-Hadi University College, 10011, Baghdad, Iraq.*
[7] *College of Petroleum Engineering, Al-Ayen University, Thi-Qar, Iraq.*
[8] *DSc in Economics, Professor, Department of Management, Ferghana Polytechnic Institute, Ferghana, Uzbekistan.*
[9] *Department of Informatics, Universitas Malikussaleh, Aceh, Indonesia.*
[10] *Kazakh National Agrarian Research University, Department of Energy Saving and Automation, Republic of Kazakhstan.*

Abstract— *Sustainable and efficient energy solutions are needed in the fast-growing energy sector. Meeting these objectives requires smart distribution networks that maximize energy utilization, eliminate losses, and improve system reliability. However, these networks' usefulness and durability depend on their ability to quickly recover from faults. Intelligent distribution networks can self-heal, which speeds up restoration and ensures energy delivery. This paper proposes a comprehensive strategy for intelligent distribution network self-healing after flaws. Restoration involves identifying and isolating the damaged area using offline and online methods. Online approaches, notably islanding, have helped restore services in the affected region. This paper presents a novel linear mathematical approach to optimize online islanding. The model estimates the boundaries of islanded microgrids and the appropriate number of microgrids for faults, enabling quick restoration. This analysis also seeks to determine the fault-affected area's system layout. A mathematical model defines the ideal arrangement in the first layer of the two-layered approach. The next layer analyzes unit participation in the intelligent distribution system, focusing on rescheduling, allocation, and organization. Additionally, the study identifies the best energy storage solutions to aid restoration. The recommended strategy uses adaptive load reduction and demand response to maximize system recovery. The mathematical model benefits from various strategies, including faster execution and better outcomes. This research advances intelligent distribution networks by combining advanced mathematical modeling, self-healing, and smart load control. These upgrades boost distribution networks' effectiveness.*

Keywords—Smart grid, energy storage solutions, self-healing, adaptive load reduction, optimization, enhanced system effectiveness.

1. INTRODUCTION

Ensuring uninterrupted provision of power to customers is of utmost importance. In radial distribution networks, energy is sent from the supply side to the consumers located at the far end of the network. In the event of a mistake occurring in the distribution network, it is imperative to promptly rectify the flaws within the system. Due to this separation, the flow of energy to certain loads may be interrupted, causing these loads to lose power [1, 2]. The integration of technical capabilities and communication infrastructure into existing networks has the potential to result in the development of networks that are more durable, dependable, and effective and that allow greater user interaction [3, 4]. This type of network implementation is usually referred to as the "smart grid." One of the most prominent features of this network is its capacity for self-healing, which enables it to automatically rectify and recover from errors. The implementation of this strategy ensures that the smart grid will operate in a safe and efficient manner. The term "self-healing" refers to the capability of the system to instantly recognize errors and limit the negative impacts of those errors by taking the required actions, thus rapidly restoring a state of normalcy and stability through the process of restoration. In the field of service recovery, several studies have been conducted under both centralized and decentralized self-healing systems. Each of these systems has its own set of advantages and disadvantages [5–9].

The implementation of self-healing mechanisms in smart grids has been the subject of study in a number of different types of research. These methods involve the employment of multi-factor methodologies, which integrate software and physical components for the purpose of exploiting vulnerabilities. There are significant improvements that can be made to the simulation of smart grids by using agent-based modeling methodologies. In specific research projects, an agent-based model has been utilized as an intelligent system for providing protection, while a fuzzy multi-agent system has been utilized as a method for providing self-healing [10–12].

Received: 20 Dec. 2023
Revised: 26 Feb. 2024
Accepted: 04 Mar. 2024
*Corresponding author:
E-mail: arabimohammedyousif@gmail.com (M.Y. Arabi)
DOI: 10.22098/joape.2024.14265.2097
Research Paper

The use of principles derived from multi-agent systems has resulted in a self-healing approach. The feeder agent, zone, switch, and distributed generation resources work together to automatically restore the network inside of these systems. The employment of artificial neural networks is crucial in these systems for anticipating the output of distribution tanks. The field of smart networks faces a huge issue in developing a self-healing control system that must be solved. Due to this attribute, power systems have the capability to autonomously restore the grid in the event of technical malfunctions. To enhance the operational adaptability of distributed power systems, the proposed designs for managing these systems aim to enable coordination between the central control system and the distributed control systems [13–17].

The efficiency of the self-healing control technology is evaluated in terms of its ability to detect faults, isolate the damaged area, restore power in the power distribution system, and identify inadequacies. In addition to this, the study investigates whether or not the system is capable of preserving the stability of microgrids while operating independently [6, 8, 18]. A novel technique is proposed for voltage regulation, with a specific focus on managing the input of reactive power. This technique is based on a complete architectural model that considers the various sun sources distributed over the terrain. Recently, demand response programs (DRPs) have become important concepts in the power and energy industries [19–21]. Integrating many types of loads, including residential, commercial, and industrial loads, into demand response programs could facilitate their integration as intelligent and adaptive loads. Researchers explore four fundamental characteristics of demand response in smart grid systems. The aspects encompassed are programs, issues, approaches, and anticipated expansions. The authors have examined the consequences of demand response programs in combination with the operation of several microgrids within active distribution networks. The energy management system (EMS) intended for individual structure microgrids includes a systematic demand response mechanism [21–23].

In research to investigate and build a smart network in public places that uses a microgrid system. Solar power generation sources, integrated heating and cooling systems, energy storage systems (ESS) and responsive loads are all parts of public space infrastructure [24, 25]. Research has also been conducted to strategically allocate different units based on companies' demand and price concerns. Another topic that has been examined is the influence of demand response on scheduled power generation [26, 27]. Furthermore, a paradigm is introduced to examine issues pertaining to real-time management challenges in smart grids. The demand response algorithms devised for this study were formulated via a multi-objective methodology. These algorithms take into account the energy expenses of residential customers in addition to the network load factor [28, 29]. A simulation for an energy management tool is being created for buildings that are connected to the electricity grid. The plan incorporates an energy center that encompasses vehicle-to-home connectivity, wind turbines, demand response systems, and diesel generators [30–32].

Recent research has focused on enhancing energy management and recovery in active distribution networks. The study examines an ideal framework for managing energy flexibility and using self-healing techniques in active distribution networks that incorporate renewable energy sources (RES) and electric vehicles (EV). This model uses demand response techniques that, along with the flexibility of renewable energy sources, make the energy distribution network more efficient and better use these sources. These studies are crucial in advancing and optimizing active distribution networks, particularly in relation to the integration of renewable energy sources [33–35].

Within the framework of the approach that was developed, a strategy that is founded on mathematical modeling is utilized in order to successfully restore service in the problematic area. Using this method, the optimal configuration of isolated microgrids and the occurrence of those configurations after a fault can be identified in an efficient manner. Following the occurrence of the problem, the affected zone is isolated, which may include turning off and then restarting particular switches. It is important to note that the switches that are linked to the main network are not taken into consideration when choosing the microgrid configuration that will be the most effective within the region that is impacted by the incident. This is done for the purpose of ensuring that the system functions independently inside the problematic area, apart from its connection to the upstream network, which prevents it from being connected to an islanded state. Establishing distinct microgrids in the issue area is the first phase of the process. These microgrids will be set up using the optimal configuration that was discovered through the use of a mathematical linear model in the first layer. Following this, the secondary layer will attempt to address the particular problem of limited involvement in the intelligent distribution system. Over the course of this phase, approaches for individual involvement are combined by employing load allocation tools and load response strategies through the utilization of a mathematical linear model. One of the most crucial aspects of this proposed technique is the utilization of an optimal approach, which significantly cuts down on the amount of time needed for problem-solving while simultaneously guaranteeing the finest potential outcome. In addition, the model incorporates a variety of technologies, such as adaptive load demand response mechanisms, diverse decentralized energy production sources, and energy storage, in order to improve the effectiveness of the operation of the recovery process. In contrast to the graphs, smart algorithms, and nonlinear models that were typically utilized in earlier research, this work takes a different approach, which is one of the innovative aspects of this work. This work, on the other hand, utilized a linear modeling approach to efficiently fix defective systems, which distinguishes it from other studies that have been conducted in this sector.

2. MODELING

The primary aspect of network self-healing following a mistake is the minimization of the self-healing period and the effectiveness of the suggested solution in restoring the highest achievable network capacities. The self-repair method should minimize the duration of network downtime and meet the customer's expectations while also being both viable and implementable. The comprehensive examination of the intelligent distribution system is the primary emphasis of this work. The performance of this system is improved, and the regulation of electricity is achieved through the utilization of a combination of distributed generation sources and energy storage. The system that is being investigated is considered to be a balanced system. The model under consideration does not take the distribution of reactive charges into account. Microturbines have a limited capacity for performance when subjected to heavy loads.

This intelligent system makes use of distributed generation and energy storage resources in order to successfully manage variations that are associated with both distributed and non-distributable generation. Controllable consumers and uncontrollable consumers are the two categories that can be used to classify consumers. A two-step strategy is suggested as a means of optimizing the units that make up the distribution system [36]. In addition, this system is incapable of managing and distributing the electricity that it receives in an equitable manner, which may result in power outages for some loads and, as a consequence, increased operational costs. In order to handle system challenges, this model makes use of a linear methodology, which demonstrates pioneering research in this field [37].

The primary objective of effective self-repair of the distribution system is to reinstate the highest load capacity using the fewest switches, a factor that must be taken into account in the proposed method of self-repair for the distribution network. Eqs. (1) and (2) display the values of the two retrieved load functions and the best switching number. In this designated strategy, it is imperative to

prioritize maximum load recovery while adhering to the network's technical constraints while minimizing the number of switches required.

$$\mathrm{f}_1 = \sum_{iNres\ S_i} \tag{1}$$

$$\mathrm{f}_2 = \mathrm{N}_{\mathrm{sw}} \tag{2}$$

The variables N_{sw}, S_i, and Nres represent the quantities of switches required to achieve the final configuration of the distribution network, the restored load, and the number of electric buses in the network, respectively. During the first stage of the process, a novel goal function is taken into account to address the challenges associated with rearrangement problems. This objective function plays a crucial role in the regulation and administration of energy distribution. The objective function takes into account crucial factors, such as allowable voltage variations, and assesses and evaluates the voltage values based on the preunit. In the objective function, a coefficient is included to represent the cost associated with allowable voltage deviations. This coefficient is expressed in terms of dollars and takes into account potential financial repercussions. The subsequent phases of this objective function independently analyze and assess the expense of collecting various loads with varying significance. The prioritization of loads takes into account factors such as mobility, interruptibility, adaptability, and the feasibility of detaching the load. An additional parameter in this goal function is the integer variable representing the number of interconnected lines. This variable is designed to minimize the interconnection of lines in the system, resulting in the formation of island microgrids. This is particularly significant in specific circumstances and for the purposes of resource management and power distribution.

$$\begin{aligned} &Min \sum_t \Big(\sum_{k,t} c^{\mathrm{delv}} \ |\Delta v_{k,t}| - \sum_k c^D p^D_{k,t}(k,t) + \\ &\sum_k c^{LS1} p^{LS1}_{k,t}(k,t) + \sum_k c^{LS2} p^{LS2}_{k,t}(k,t) + \\ &\sum_k c^{LS3} p^{LS3}_{k,t}(k,t) + \sum_k c^{LS4} p^{LS4}_{k,t}(k,t) + \sum_{k,j}(k,j) \Big) \end{aligned} \tag{3}$$

During the initial semester, costs are incurred as a consequence of voltage fluctuations that exceed the rated voltage. These costs are calculated using the absolute value function. Because if the absolute value is not used, the goal function tries to minimize and go to the smallest voltage allowed. It is necessary to find a suitable replacement to stop the model from becoming nonlinear because the absolute value function introduces nonlinearity. The purpose of incorporating the absolute value in the initial term of the model is to ensure that the model focuses on voltages that exceed the minimum permissible threshold. Here, the voltage deviation term is substituted with the sum of two positive variables, Xp(k,t) and Xn(k,t), in the first term of Eq. (4), maintaining the same nominal value. By utilizing Eq. (5), these two variables have the ability to transform the modeling of voltage deviation values from a non-linear to a linear form.

$$\begin{aligned} &Min \sum_t \Big(\sum_{k,t} c^{\mathrm{delv}} \ (X_p(k,t) + X_n(k,t)) - \\ &\sum_k c^D p^D_{k,t}(k,t) + \sum_k c^{|SS|} p^{LS1}_{k,t}(k,t) + \\ &\sum_k c^{LS2} p^{LS2}_{k,t}(k,t) + \sum_k c^{LS3} p^{LS3}_{k,t}(k,t) + \\ &\sum_k c^{LS4} p^{LS4}_{k,t}(k,t) + \sum_{k,j} X(k,j) \Big) \end{aligned} \tag{4}$$

$$\Delta \mathrm{V}_{k,t} = (X_p(k,t) - X_n(k,t)) \tag{5}$$

Eq. (6) displays the permissible voltage value for each defective passage.

$$1 - \Delta V \le \mathrm{V}_{k,t} \le 1 + \Delta V \tag{6}$$

The equations for the distribution of active and reactive AC loads are represented by Eqs. (7) and (8), correspondingly. These two relations exhibit a high degree of non-linearity, which leads to the solver being unable to find a solution. Therefore, in the subsequent formulation, these two relations will be expressed as linear equations.

$$\begin{aligned} &P_{k,j,t} = \\ &X_{k,j} \left(\mathrm{V}_{k,t} \sum_j \mathrm{V}_{j,t} \left(G_{K,J} \cos\theta_{k,t} + B_{K,J} \sin\theta_{k,t} \right) \right), \ \forall k \end{aligned} \tag{7}$$

$$\begin{aligned} &Q_{k,j,t} = \\ &X_{k,j} \left(\mathrm{V}_{k,t} \sum_j \mathrm{V}_{j,t} \left(G_{K,J} \sin\theta_{kj,t} - B_{K,J} \cos\theta_{kj,t} t \right) \right), \ \forall k \end{aligned} \tag{8}$$

Because the load distribution equations in Eqs. (7) and (8) are non-linear, these two relations are linearized. In order to linearize, the following assumptions must hold: The voltage consistently remains in close proximity to the nominal value. Given the minor difference in voltage angles, we can approximate the sine of θ as equal to θ and its cosine as equal to one. Thus, the voltage of a bus can be represented in the following manner:

$$V_{k,t} = 1 + \Delta V \tag{9}$$

The voltage fluctuations must remain within the permissible range. Therefore, based on Eq. (9), Eqs. (7) and (8) undergo the following modifications:

$$\begin{aligned} &P_{k,j,t} = \\ &\sum_j \left((1 + \mathrm{V}_{k,t} + \mathrm{V}_{j,t}) G_{k,j} + B_{k,j} \cdot \theta_{kj,t} \right), \ \forall k \end{aligned} \tag{10}$$

$$\begin{aligned} &Q_{k,j,t} = \\ &\sum_j (1 + \mathrm{V}_{k,t} + \mathrm{V}_{j,t}) \left(G_{k,j} \theta_{kj,t} - B_{k,j} \right), \ \forall k \end{aligned} \tag{11}$$

Eqs. (10) and (11) remain non-linear as a result of the multiplication of two variables. Given the anticipated minuscule value of the product of $\Delta \mathrm{V}_{j,t}.\theta_{kj,t}$ and $\Delta \mathrm{V}_{k,t}.\theta_{kj,t}$, the nonlinear terms are thus eliminated from Eqs. (8) and (9). As a result, Eqs. (12) and (13) represent linear equations for load distribution.

$$\begin{aligned} &P_{k,j,t} = \\ &\sum_j \left((1 + \mathrm{V}_{k,t} + \mathrm{V}_{j,t}) G_{k,j} + B_{k,j} \cdot \theta_{kj,t} \right), \ \forall k \end{aligned} \tag{12}$$

$$\begin{aligned} &Q_{k,j,t} = \\ &\sum_j \left(G_{k,j} \theta_{kj,t} - (1 + \Delta \mathrm{V}_{k,t} + \Delta \mathrm{V}_{j,t}) B_{k,j} \right), \ \forall k \end{aligned} \tag{13}$$

Eqs. (12) and (13) contain non-linear active and reactive load distribution equations, as a result of the multiplication by $X_{k,j}$. In order to linearize these equations, it is imperative to eliminate the variable $X_{k,j}$ from the load distribution equations. The binary variable should be multiplied by the active and reactive injection power. The load distribution equations in this scenario can be readily linearized. Within these equations, the variable M represents a substantial numerical value.

$$P_{k,j,t} \le M \times \mathrm{X}_{k,j} \tag{14}$$

$$P_{k,j,t} \ge -M \times \mathrm{X}_{k,j} \tag{15}$$

Eq. (16) represents the equilibrium of active power in each bus, while Eq. (17) represents the equilibrium of reactive power in each bus.

$$P_{kj,t} = P^{G}_{k,t} + P^{E}_{k,t} - P^{D}_{k,t} + P^{WT}_{k,t} + P^{pV}_{k,t} + P^{Es}_{i,t} - P^{Es}_{i,t} \tag{16}$$

$$Q_{kj,t} = q^{G}_{k,t} - q^{D}_{k,t} + q^{WT}_{k,t} + q^{PV}_{k,t} \tag{17}$$

As per Eq. (18), the apparent power of each production source must not beyond the permissible limit:

$$\left(P^{G}_{k,t}\right)^2 + \left(q^{G}_{k,t}\right)^2 \leq \mathrm{S}^{max\ 2}_{k} \tag{18}$$

Eq. (18) is a non-linear equation, which significantly prolongs the problem-solving time. To address this, the polygon-based linearization method is employed to linearize Eq. (19). The radius of the circle is chosen from the polygon s, where x represents the number of edges of the polygon for linearization. Consequently, the linearized Eqs. (19) to (22) take the place of the non-linear Eq. (16).

$$S_k = S^{max}_{k} \sqrt{\frac{\frac{2\pi}{\eta}}{sin}} \left(\frac{2\pi}{\eta}\right) \tag{19}$$

$$-\sqrt{3}\left(P^{G}_{k,t} + S_k\right) \leq q^{G}_{k,t} \leq -\sqrt{3}\left(P^{G}_{k,t} - S_k\right) \tag{20}$$

$$\frac{-\sqrt{3}}{2} S_k \leq q^{\circ}_{k,t} \leq \frac{\sqrt{3}}{2} S_k \tag{21}$$

$$\sqrt{3}\left(p^{G}_{k,t} - S_k\right) \leq q^{G}_{k,t} \leq \sqrt{3}\left(p^{G}_{k,t} + S_k\right) \tag{22}$$

Battery storage enhances the distribution system by storing energy during periods of low demand and by discharging and minimizing the extraction of energy during periods of high demand. Regarding Eq. (23), the specified boundaries for both the process of charging and discharging are outlined.

$$-P^{c,max}_{k} \cdot \lambda_{k,t} \leq \mathrm{p}^{E}_{k,t} \leq \mathrm{p}^{dch,max}_{k} \cdot \phi_{k,t} \tag{23}$$

The battery can only undergo charging or discharging processes at any given moment, as specified by the constraint outlined in Eq. (24).

$$\lambda_{k,t} + \phi_{k,t} \leq 1 \tag{24}$$

Eq. (25) represents the state of battery charge, while Eq. (26) represents the lowest and maximum state of battery charge.

$$\mathrm{sOC}_{k,t} = \mathrm{SOC}_{k,t-1} - \frac{T}{\mathrm{EC}_k}\left(\phi_{k,t} P^{E}_{k,t} \pi_a^{-1} + \lambda_{k,t} P^{E}_{k,1} \pi_c\right) \tag{25}$$

$$0 \leq \mathrm{SOC}_{k,t} \leq \mathrm{SOC}^{max}_{k} \tag{26}$$

Although there are some limitations in linear models, microturbine modeling has primarily relied on linear models as one of the proposed methods. This approach aims to reduce complexity and simplify the modeling process, ensuring the ability to obtain a convergent response. By avoiding non-convex nonlinear equations, the linear model allows for a more manageable and predictable analysis. The issue might be characterized as a mixed integer linear programming difficulty within the GEMS software. The power output of the microturbine unit i at time t must fall within the specified operating range as defined in Eq. (27). The lowest and maximum operating range of the microturbine vary depending on the time. The values of these two variables may not necessarily be equivalent to d and z. The maximum operating limit is specified in Eqs. (28) and (29). Eq. (30) represents the mathematical model for the upper and lower limits of the ramp of the microturbine.

$$\underline{pg}_{(k,t)} \leq pg \leq \overline{pg}_{(k,t)} \tag{27}$$

$$\overline{pg}_{(k,t)} \leq pg^{\max\ \max}_{(k,t)} \left[U_{k,t} - Z_{k,t+1}\right] + \mathrm{SD}_k Z_{k,t+1} \tag{28}$$

$$\overline{pg}_{(k,t)} \leq \mathrm{pg}_{(k,t-1)} + R_{k,t} u_{k,t-1} + SU_k y_{k,t} \tag{29}$$

$$\underline{pg}_{(k,t)} \geq \mathrm{pg}^{min}_{(k,t)} u_{k,t} \tag{30}$$

$$\underline{pg}_{(k,t)} \leq \mathrm{pg}_{(k,t-1)} + \mathrm{RD}_{k,t} u_{k,t-1} + \mathrm{SU}_k Z_{k,t} \tag{31}$$

Eqs. (32) and (33) specify the expenses associated with initiating and ceasing operations of microturbines. These costs are subsequently employed in Eqs. (3) and (4) to determine the target function and plan the deployment of microturbines.

$$\mathrm{STC}_{(K,T)} = \mathrm{SU}_K y_{k,t} \tag{32}$$

$$\mathrm{SDC}_{(K,T)} = \mathrm{SD}_K Z_{k,t} \tag{33}$$

The state of unit i at time t is determined by the input $u_{i,t}$. The initiation and termination of the microturbine's operation is dictated by variables $y_{i,t}$ and $z_{i,t}$. The constraints associated with the activation and deactivation of microturbines are most accurately explained by Eqs. (34) and (35). However, the inclusion of these two equations renders the model non-linear. Eqs. (34) to (36) are employed as a substitute for Eq. (32) in order to linearize the limit of the minimum shutdown time. Eq. (37) imposes a constraint on the microturbine's operation, specifically on its ability to start up and shut down. This constraint is based on the microturbine's past on and off states. Eq. (38) demonstrates that the microturbine transitions between the on and off states at time t, and it is not possible for both states to be active simultaneously. Eq. (36) demonstrates that a, b, and c are all binary variables.

$$\left(y_{k,t-1} - \mathrm{UT}_k\right) \times \left(u_{k,t-1} - u_{k,t}\right) \geq 0 \tag{34}$$

$$\left(y_{k,t-1} - \mathrm{DT}_k\right) \times \left(u_{k,t-1} - u_{k,t}\right) \leq 0 \tag{35}$$

$$y_{k,t} - Z_k = u_{k,t} - u_{k,t-1} \tag{36}$$

$$y_{k,t} + z_k \leq 1 \tag{37}$$

$$y_{k,t},\ z_{k,t},\ u_{k,t} \in \{0,1\} \tag{38}$$

Eqs. (39) to (43) represent the lower bound for the duration that each microturbine remains operational, whereas Eqs. (44) to

(46) indicate the minimum duration for which each microturbine remains inactive.

$$\sum_{t=1}^{s}(1-u_{k,t})=0 \tag{39}$$

$$\begin{array}{l}\sum_{t=T}^{U_k-1}\geq \mathrm{UT}_k y_{k,r},\\ \forall\Gamma=\xi_k+1\ldots\mathrm{T}-\mathrm{DT}_k+1\end{array} \tag{40}$$

$$\begin{array}{l}\sum_{t=\Gamma}^{T}u_{k,t}-y_{k,t}\geq 0,\\ \forall T=T-\mathrm{DT}_k+2\ldots\mathrm{T}\end{array} \tag{41}$$

$$\xi_k=min\left\{T,\ \left(\mathrm{UT}_k-U_k^0\right)u_{k,t}\right\} \tag{42}$$

$$\sum_{t=1}^{k}u_{k,t}=0 \tag{43}$$

$$\begin{array}{l}\sum_{t=\Gamma}^{\Gamma+DT_T-1}(1-u_{k,t})\geq D_1 z_{k,\Gamma},\\ \forall T=\xi_k+1\ldots T-D_k+1\end{array} \tag{44}$$

$$\begin{array}{l}\sum_{t=\Gamma}^{T}1-u_{k,t}z_{k,t}\geq 0,\\ \forall\Gamma=T-\mathrm{DT}_\Gamma+2\ldots\mathrm{T}\end{array} \tag{45}$$

$$\xi=min\left\{T_2\left(\mathrm{DT}_k-S_k^0\right)\left[1-u_{k,t-0}\right]\right\} \tag{46}$$

The load power in each bus $p_{i,t}^{D}$ is determined by the cumulative power consumption of residential devices, which are assigned different priorities, as stated in relation 47. The load collector's role is to aggregate the power from devices with varying priorities across different buses, and continuously provide the total power of the distribution system for each priority to the management control section of the distribution system. Eq. (48) demonstrates that the aggregate load of the highest priority devices in each bus is lower than the combined power of the highest priority devices in all residences within each bus. Eqs. (49) and (50) illustrate the boundaries for load removal in the case of loads with priority 2 and 3, whereas Eq. (49) demonstrates the limits for disconnecting unmanageable loads.

$$\begin{array}{l}p_{k,t}^{D}=\ \mathrm{ploadl}\ _{k,t}^{D}+\ \mathrm{pload}\ _{k,t}^{D}+\\ \mathrm{pload}\ _{k,t}^{D}+\ \mathrm{pload}\ _{k,t}^{D}\end{array} \tag{47}$$

$$0\leq \mathrm{p}_{k,t}^{LSI}\leq\ \mathrm{ploadl}\ _{k,t}^{D} \tag{48}$$

$$0\leq p_{k,t}^{LS3}\leq\ \mathrm{pload}\ 3_{k,t}^{D} \tag{49}$$

$$0\leq p_{k,t}^{LS3}\leq\ \mathrm{pload}\ 3_{k,t}^{D} \tag{50}$$

$$0\leq p_{k,t}^{LS4}\leq\ \mathrm{pload}\ 4_{k,t}^{D} \tag{51}$$

Eq. (52) facilitates the creation of efficient microgrids in the system by establishing active and reactive load distribution connections. Furthermore, they also ensure the radial nature of the system. The value of N_T also represents the upper limit for the number of interconnected lines, as calculated by Eq. (53). Eq. (53) states that if there is a loop inside the fault occurrence area, one of the open lines of the system must be chosen within this loop. This ensures that the system remains in a radial condition and prevents any loops from forming in the system.

Table 1. Information on scattered production sources and batteries.

Wind Turbine		Energy storage system				Photovoltaic	
location	Minimum charge	location	Minimum charge	power	Initial charge	location	power
3	20						
8	60	5	0.1	100	0.6	6	40
12	60	10	0.1	100	0.8	10	50
15	50	14	0.1	150	0.7	19	50
17	40	18	0.1	150	0.5	27	60
22	40	20	0.1	250	0.9		
26	80	32	0.1	250	0.7		
30	70						

$$\sum_{k,j}x\left(k,j\right)\leq \mathrm{N}_T \tag{52}$$

$$N_T=\sum_k \mathrm{N}_k-\sum_u \mathrm{N}_u \tag{53}$$

However, after the rearrangement is completed, the matter of unit involvement in the new system must be addressed and resolved. During this stage, the planning is conducted for the distribution and storage of production sources that are spread out, and the quantity of load harvesting is determined. The objective function of the second layer incorporates all the significant objectives involved in modeling the individual participation problem. The objective function 52 represents the cumulative costs associated with production, pollution, startup, and shutdown of microturbines from the first to fourth semesters. The fifth term corresponds to the clients' sales profit. During semesters 6 to 9, the expenses associated with acquiring priority loads 1 to 3 and load interruption are displayed. The 11th and 12th terms display the expenses incurred in purchasing electricity from the upstream network and the revenue generated from selling electricity to the upstream network. Some studies assume the production cost of microturbines to be a quadratic function. However, in order to decrease the computing burden, a linear model has been employed for the production cost function of microturbines. Thus, the objective function has been modified by replacing the nonlinear term with a linear term, resulting in Eq. (2) representing a linear model. Additionally, a linear coefficient has been incorporated into the goal function to account for the cost of pollution.

$$\begin{array}{l}Min\sum_t\left(\sum_{k,t}c^{\mathrm{delv}}\ |\Delta v_{k,t}|-\sum_k c^D p_{k,t}^D\left(k,t\right)+\right.\\ \sum_k c^{LS1}p_{k,t}^{LS1}\left(k,t\right)+\sum_k c^{LS2}p_{k,t}^{LS2}\left(k,t\right)+\\ \left.\sum_i c^{LS2}p_{i,t}^{LS2}+\sum_i c^{LS3}p_{i,t}^{LS3}+\sum_i c^{LC}p_{i,t}^{LC}\right)c_t^t\mu\end{array} \tag{54}$$

Eqs. (55) and (56) illustrate the allocation of active and reactive loads. However, in this context, $x\left(k,j\right)$ does not function as a variable. Instead, it reflects the state of the system lines gained from step one. Hence, Eqs. (12) and (13) are not required to linearize these two relations.

$$\begin{array}{l}p_{k,j,t}=x\left(k,j\right)\times\\ \sum_j\left(\left(1+\Delta\mathrm{v}_{k,t}+\Delta\mathrm{v}_{j,t}\right)G_{k,j}+B_{k,j,t}\cdot\theta_{kj,t}\right),\ \forall k\end{array} \tag{55}$$

$$\begin{array}{l}Q_{k,j,t}=x\left(k,j\right)\times\\ \sum\left(G_{j,t}\theta_{kg,t}-\left(1+\Delta\mathrm{v}_{k,t}+\Delta\mathrm{v}_{j,t}\right)B_{k,j}\right),\ \forall k\end{array} \tag{56}$$

3. RESULTS

The information shown in Table 1 presents information regarding the quantity of scattered production sources and energy storage systems in the system that was studied, as well as their placement. It is made up of eight wind turbines, four solar sources, and six energy storage units as its components. Not only that, but Table 2 contains information that is particularly pertinent to microturbines. According to the system that is being investigated, it is presumed that the amount of electricity that is consumed by each residential

Table 2. Information on scattered production sources and batteries.

MT location	Power maximum	Incremental rate	Discount rate	Minimum on time	Minimum shut-down time	Initial state of microturbines	Start-up and shut-down costs of microturbines
12	750	200	200	1.5	1.5	1	5
15	750	200	200	1.5	1.5	1	5
18	800	250	250	1.5	1.5	0	5
20	100	100	100	1.5	1.5	0	5
23	750	200	200	1.5	1.5	0	5
25	650	200	200	1.5	1.5	1	5
29	650	200	200	1.5	1.5	1	5

Table 3. Information on scattered production sources and batteries.

Parameters	Amount	Parameters	Amount
C^G	0.2	C^{LS1}	4.5
C^D	0.38	C^{LS2}	3.5
C^{emi}	0.08	C^{LS3}	2.8
σ_i	0.009	C^{LS4}	6

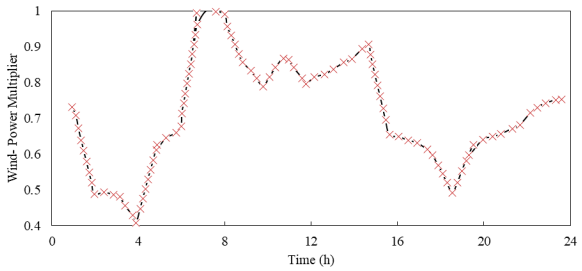

Fig. 1. Wind power coefficients.

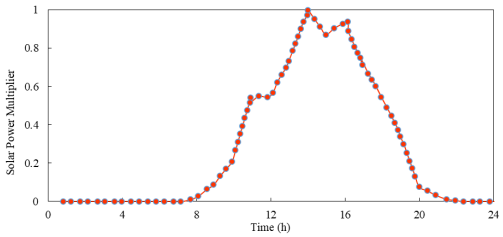

Fig. 2. Solar power coefficients.

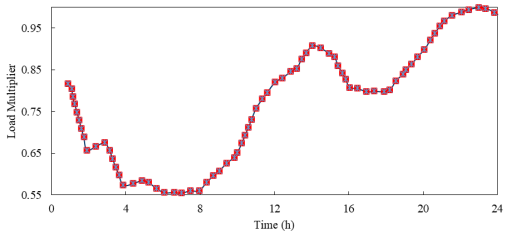

Fig. 3. Load coefficients.

house is 12 kW. It is possible to divide the intelligent gadgets that are present in every home into three distinct categories: devices that are adjustable, devices that are interruptible, and devices that are detachable. Home appliances that have a power rating of 1.8 kW or higher are considered to be uncontrolled types of appliances. A total power capacity of 4.5 kW is deemed to be available for devices with first priority, which includes mobile loads, and this capacity is measured for each individual residence. There is a capacity of 3.2 kW for devices that have second priority, which includes loads that are affected by interruptions.

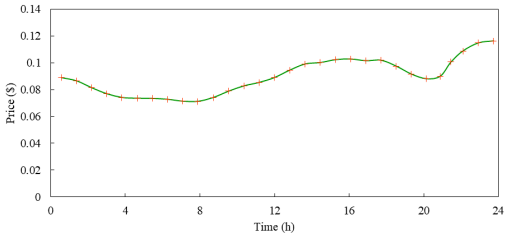

Fig. 4. Energy prices in 24 hours.

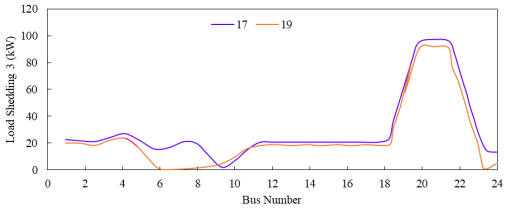

Fig. 5. Third priority load shedding.

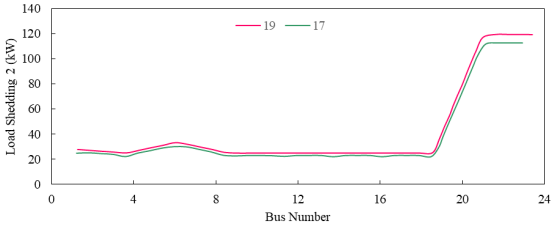

Fig. 6. Second priority load shedding.

The capacity of devices with third priority, which includes loads that can be adjusted, is determined to be 2.5 kW. The data of microturbines is presented in Table 3.

Figs. 1 to 6 display the coefficients for wind, solar, load, and energy price. In order to evaluate the suggested model in the initial layer, a fault occurring between buses 7 and 8 is taken into account. By separating the connection between busses 7 and 8, the faulty area has been divided into four distinct island microgrids. The initial observation on the outcomes is that the microturbines 17 and 24, which are connected to the upstream grid, do not produce any power. Fig. 6 illustrates the energy price at 17 and 19 hours, indicating that during these two hours, the energy price is below $0.1 per kilowatt-hour. Given that the production cost of microturbines is $0.1/kWh, the program's inclination is to procure electricity from the upstream grid rather than manufacturing microturbines in order to minimize operational expenses.

The battery is charged to 5 units because the minimum battery charge is 40 kilowatts. The initial battery charge state of 5 is deemed to be 20 kilowatts. As a result of the minimum battery charge requirement, battery 5 reaches its lowest charge by receiving a charge of 20.7 kilowatts at 17:00. All the remaining batteries

are depleted until they reach the minimum level of battery charge. There were no power outages during the 17th and 19th hours. In order to minimize operational expenses, the load will be reduced to 958.5 kilowatts at 17:00 and 1100.6 kilowatts at 19:00.

Figs. 5 and 6 display the quantity of selection for the third and second priority loads on each bus, respectively. As part of the load response program, the first priority loads are given the utmost importance and have the highest cost associated with their collection. However, no first priority loads were selected at 17 and 19 hours.

Third priority loads are assigned the lowest value as a result of their diminished significance. Thus, based on Fig. 5, the highest level of harvesting has happened within these specific time periods. Based on Fig. 6, the load of the second priority in various buses is significantly lower. Fig. 6 shows that busses 24 and 25 have the highest sampling rate due to their substantial load.

4. CONCLUSION

The process of restoring the distribution system after an error has occurred is one of the procedures that are included in the self-repair functionality of intelligent distribution systems. The process of recovery is comprised of two stages: the first stage is the identification of the defect, and the second stage is the involvement of the unit. Academics that are interested in finding a solution to the rearrangement problem in large distribution systems face a considerable challenge in the form of increased execution time. In the past, researchers have frequently utilized graph theory, smart algorithms, and non-linear models in order to solve the problem of rearrangement. On the other hand, these methods have led to much higher execution times, which has rendered them nearly impossible to use in operational settings. In this study, a novel linear model is presented as a solution to the problem of post-error rearrangement. Through the utilization of mathematical solvers, the strategy considerably reduces the amount of time required to solve the problem and guarantees the achievement of the best possible solution. The primary layer is responsible for transforming the problematic area into one or more isolated microgrids by utilizing the approach that was described prior to this. This is a huge advantage of the technique that has been described since it makes it possible to create ideal isolated microgrids in real time once a fault event has occurred. Furthermore, the problem of unit involvement in an intelligent distribution system has been solved by the adoption of a linear model in the second tier. This model makes use of the redesigned arrangement that was obtained from the system's initial stage. Both distributable and non-distributable production sources and storages, in addition to load response technologies, are utilized by the intelligent structure that is described in this article. Adjustable loads, interruptible loads, and movable loads are the three main categories that the load response tool recognizes as belonging to controlled loads. The self-repair mode of the system also promotes economic optimization, which results in lower costs. This is accomplished through the exploitation of load response plans and the resources that are already present in the system. The numerical findings that were presented, in conjunction with the comparison to techniques that are already in use, guarantee that the proposed method will perform at its highest possible level.

REFERENCES

[1] K. H. M. Azmi, N. A. M. Radzi, N. A. Azhar, F. S. Samidi, I. T. Zulkifli, and A. M. Zainal, "Active electric distribution network: applications, challenges, and opportunities," *IEEE Access*, vol. 10, pp. 134655–134689, 2022.

[2] J. Wei, A. Chammam, J. Feng, A. Alshammari, K. Tehranian, N. Innab, W. Deebani, and M. Shutaywi, "Power system monitoring for electrical disturbances in wide network using machine learning," *Sustainable Comput. Inf. Syst.*, vol. 42, p. 100959, 2024.

[3] V. H. de Souza, W. Satyro, J. C. Contador, L. F. Pinto, and M. C. Mitidiero, "The technology analysis model-tam 4.0 for implementation of industry 4.0," *Int. J. Ind. Eng. Manage.*, vol. 14, no. 4, pp. 271–281, 2023.

[4] E. J. Oughton, Z. Frias, S. van der Gaast, and R. van der Berg, "Assessing the capacity, coverage and cost of 5g infrastructure strategies: Analysis of the netherlands," *Telematics Inf.*, vol. 37, pp. 50–69, 2019.

[5] W. Altalabani and Y. Alaiwi, "Optimized adaptive pid controller design for trajectory tracking of a quadcopter," 2022.

[6] J.-D. Hong, J. Mwakalonge, and K.-Y. Jeong, "Design of disaster relief logistics network system by combining three data envelopment analysis-based methods," *Int. J. Ind. Eng. Manage.*, vol. 13, no. 3, pp. 172–185, 2022.

[7] L. F. F. De Almeida, L. A. M. Pereira, A. C. Sodré, L. L. Mendes, J. J. Rodrigues, R. A. Rabelo, A. M. Alberti, *et al.*, "Control networks and smart grid teleprotection: Key aspects, technologies, protocols, and case-studies," *IEEE Access*, vol. 8, pp. 174049–174079, 2020.

[8] E. Shittu, A. Tibrewala, S. Kalla, and X. Wang, "Meta-analysis of the strategies for self-healing and resilience in power systems," *Adv. Appl. Energy*, vol. 4, p. 100036, 2021.

[9] N. Nedjah, K. H. Cardoso, and L. de Macedo Mourelle, "An efficient distributed approach for a self-healing smart grid using minimal spanning tree," *Int. J. Energy Res.*, vol. 45, no. 10, pp. 15049–15084, 2021.

[10] S. S. Binyamin and S. Ben Slama, "Multi-agent systems for resource allocation and scheduling in a smart grid," *Sens.*, vol. 22, no. 21, p. 8099, 2022.

[11] L. Rafferty, *Agent-based modeling framework for adaptive cyber defence of the Internet of Things*. PhD thesis, 2022.

[12] K. Kotis, S. Stavrinos, and C. Kalloniatis, "Review on semantic modeling and simulation of cybersecurity and interoperability on the internet of underwater things," *Future Internet*, vol. 15, no. 1, p. 11, 2022.

[13] A. A. Shobole and M. Wadi, "Multiagent systems application for the smart grid protection," *Renewable Sustainable Energy Rev.*, vol. 149, p. 111352, 2021.

[14] A. Sujil, J. Verma, and R. Kumar, "Multi agent system: concepts, platforms and applications in power systems," *Artif. Intell. Rev.*, vol. 49, pp. 153–182, 2018.

[15] M. Chen, "A multi-agent system design and implementation for flexible network management," 2018.

[16] I. Loeser, M. Braun, C. Gruhl, J.-H. Menke, B. Sick, and S. Tomforde, "Towards organic distribution systems–the vision of self-configuring, self-organising, self-healing, and self-optimising power distribution management," *ArXiv Prepr. ArXiv:2112.07507*, 2021.

[17] N. Dkhili, J. Eynard, S. Thil, and S. Grieu, "A survey of modelling and smart management tools for power grids with prolific distributed generation," *Sustainable Energy Grids Networks*, vol. 21, p. 100284, 2020.

[18] D. Sarathkumar, M. Srinivasan, A. A. Stonier, R. Samikannu, N. R. Dasari, and R. A. Raj, "A technical review on self-healing control strategy for smart grid power systems," in *IOP Conf. Ser. Mater. Sci. Eng.*, vol. 1055, p. 012153, IOP Publishing, 2021.

[19] N. Shaukat, S. Ali, C. Mehmood, B. Khan, M. Jawad, U. Farid, Z. Ullah, S. Anwar, and M. Majid, "A survey on consumers empowerment, communication technologies, and renewable generation penetration within smart grid," *Renewable Sustainable Energy Rev.*, vol. 81, pp. 1453–1475, 2018.

[20] S. Haghifam, M. Dadashi, K. Zare, and H. Seyedi, "Optimal operation of smart distribution networks in the presence of demand response aggregators and microgrid owners: A multi follower bi-level approach," *Sustainable Cities Soc.*, vol. 55, p. 102033, 2020.

[21] H. Farzaneh, L. Malehmirchegini, A. Bejan, T. Afolabi, A. Mulumba, and P. P. Daka, "Artificial intelligence evolution in smart buildings for energy efficiency," *Appl. Sci.*, vol. 11, no. 2, p. 763, 2021.

[22] S. E. Ahmadi and N. Rezaei, "A new isolated renewable based multi microgrid optimal energy management system considering uncertainty and demand response," *Int. J. Electr. Power Energy Syst.*, vol. 118, p. 105760, 2020.

[23] S. Vuddanti and S. R. Salkuti, "Review of energy management system approaches in microgrids," *Energies*, vol. 14, no. 17, p. 5459, 2021.

[24] S. Alrashed, "Key performance indicators for smart campus and microgrid," *Sustainable Cities Soc.*, vol. 60, p. 102264, 2020.

[25] C. Ma, "Smart city and cyber-security; technologies used, leading challenges and future recommendations," *Energy Rep.*, vol. 7, pp. 7999–8012, 2021.

[26] A. R. Jordehi, "Optimisation of demand response in electric power systems, a review," *Renewable Sustainable Energy Rev.*, vol. 103, pp. 308–319, 2019.

[27] K. Alshehri, J. Liu, X. Chen, and T. Başar, "A game-theoretic framework for multiperiod-multicompany demand response management in the smart grid," *IEEE Trans. Control Syst. Technol.*, vol. 29, no. 3, pp. 1019–1034, 2020.

[28] T. Nasir, S. S. H. Bukhari, S. Raza, H. M. Munir, M. Abrar, H. A. u. Muqeet, K. L. Bhatti, J.-S. Ro, and R. Masroor, "Recent challenges and methodologies in smart grid demand side management: State-of-the-art literature review," *Math. Probl. Eng.*, vol. 2021, pp. 1–16, 2021.

[29] U. Assad, M. A. S. Hassan, U. Farooq, A. Kabir, M. Z. Khan, S. S. H. Bukhari, Z. u. A. Jaffri, J. Olah, and J. Popp, "Smart grid, demand response and optimization: a critical review of computational methods," *Energies*, vol. 15, no. 6, p. 2003, 2022.

[30] A. Alsharif, C. W. Tan, R. Ayop, A. Dobi, and K. Y. Lau, "A comprehensive review of energy management strategy in vehicle-to-grid technology integrated with renewable energy sources," *Sustainable Energy Technol. Assess.*, vol. 47, p. 101439, 2021.

[31] Y. Zhou, S. Cao, J. L. Hensen, and P. D. Lund, "Energy integration and interaction between buildings and vehicles: A state-of-the-art review," *Renewable Sustainable Energy Rev.*, vol. 114, p. 109337, 2019.

[32] S. K. Rathor and D. Saxena, "Energy management system for smart grid: An overview and key issues," *Int. J. Energy Res.*, vol. 44, no. 6, pp. 4067–4109, 2020.

[33] M. A. Gilani, A. Kazemi, and M. Ghasemi, "Distribution system resilience enhancement by microgrid formation considering distributed energy resources," *Energy*, vol. 191, p. 116442, 2020.

[34] M. Stecca, L. R. Elizondo, T. B. Soeiro, P. Bauer, and P. Palensky, "A comprehensive review of the integration of battery energy storage systems into distribution networks," *IEEE Open J. Ind. Electron. Soc.*, vol. 1, pp. 46–65, 2020.

[35] M. W. Khan, J. Wang, M. Ma, L. Xiong, P. Li, and F. Wu, "Optimal energy management and control aspects of distributed microgrid using multi-agent systems," *Sustainable Cities Soc.*, vol. 44, pp. 855–870, 2019.

[36] P. Chetthamrongchai, O. G. Stepanenko, N. R. Saenko, S. Y. Bakhvalov, G. Aglyamova, and A. H. Iswanto, "A developed optimization model for mass production scheduling considering the role of waste materials," *Int. J. Ind. Eng. Manage.*, vol. 13, no. 2, pp. 135–144, 2022.

[37] R. C. Sabioni, J. Daaboul, and J. Le Duigou, "Joint optimization of product configuration and process planning in reconfigurable manufacturing systems," *Int. J. Ind. Eng. Manage.*, vol. 13, no. 1, pp. 58–75, 2022.